

LIGHTWEIGHT ERROR MITIGATION STRATEGIES FOR POST-TRAINING N:M ACTIVATION SPARSITY IN LLMS

Shirin Alanova
equal contribution

Kristina Kazistova
equal contribution

Ekaterina Galaeva
equal contribution

Alina Kostromina
equal contribution

Vladimir Smirnov

Redko Dmitry

Alexey Dontsov

Maxim Zhelnin

Evgeny Burnaev

Egor Shvetsov

ABSTRACT

The demand for efficient large language model (LLM) inference has intensified the focus on sparsification techniques. While semi-structured (N:M) pruning is well-established for weights, its application to activation pruning remains under-explored despite its potential for dynamic, input-adaptive compression and reductions in I/O overhead. This work presents a comprehensive analysis of methods for post-training N:M activation pruning in LLMs. Across multiple LLMs, we demonstrate that pruning activations enables superior preservation of generative capabilities compared to weight pruning at equivalent sparsity levels. We evaluate lightweight, plug-and-play error mitigation techniques and pruning criteria, establishing strong hardware-friendly baselines that require minimal calibration. Furthermore, we explore sparsity patterns beyond NVIDIA’s standard 2:4, showing that the 16:32 pattern achieves performance nearly on par with unstructured sparsity. However, considering the trade-off between flexibility and hardware implementation complexity, we focus on the 8:16 pattern as a superior candidate. Our findings provide both effective practical methods for activation pruning and a motivation for future hardware to support more flexible sparsity patterns. Our code is available [here](#).

1 INTRODUCTION

The expanding capabilities of Large Language Models (LLMs) have driven enormous demand for efficient AI inference. A common rule of thumb states that inference serving speed for a dense model with N parameters scales as $\propto 1/\sqrt{N}$ (Erdil, 2025). Accelerating inference typically involves either reducing numerical precision via quantization to mitigate memory bottlenecks and enable faster arithmetic (Shvetsov et al., 2024) or sparsification to reduce the number of parameters (Maximov et al., 2025). Sparsity improves LLM efficiency in two key ways: (1) by reducing computation, and (2) by reducing I/O traffic for transferring parameters between memory and compute units – a major bottleneck during inference.

Weights vs. Activations. While sparse weights and activations offer identical theoretical FLOPs (floating point operations count), their practical implications differ. Weight sparsity enables static compression, efficiently reducing model storage and memory bandwidth. However, its static nature often causes irreversible model degradation. In contrast, activation sparsity is dynamic and input-adaptive, preserving model capacity, which we demonstrate in our work.

Sparsity in LLMs. Naturally, pruning is most effective when the values to be pruned already have low magnitudes or are zero, which is often the case for some LLMs’ intermediate representations (Liu et al., 2023), especially due to the ReLU activation function in MLP blocks (Mirzadeh et al., 2023). Even if a model was trained with a non-ReLU activation function, we can still perform

relufication Song et al. (2024b) to induce sparsity. This makes activation sparsification a natural choice for enhancing the model’s performance.

Accelerating LLMs with sparse activations. Indeed, recent results demonstrated that activation sparsification supported by specialized software can increase the model’s vector by matrix multiplication during the LLM decoding stage up to $2\times$ times (Song et al., 2024b;a; Liu et al., 2024; Lee et al., 2024). The idea behind such approaches is relatively straightforward - if a vector has many zeroes, we can disregard corresponding columns in a weight matrix W on the fly. However, as batch size grows beyond *one*, it becomes challenging to gain benefits (Shrestha et al., 2025). Moreover, most previous methods mainly rely on sparsity induced only by activation functions (Mirzadeh et al., 2023) in MLP blocks.

Semi-structured N:M sparsity for activations, where each N elements out of a sub-vector of M are zeroes, would provide computational gains beyond single vector \times matrix computations. This approach is a trade-off between the performance retention of unstructured pruning (Zhu et al., 2016; Paul et al., 2022) and the hardware-friendly acceleration of structured pruning (Liu et al., 2017; Molchanov et al., 2019), motivating its use for efficient inference (Hubara et al., 2021). Several works demonstrate that 2:4 sparsity patterns for activations, combined with Squared-ReLU, can accelerate transformer training (Haziza et al., 2025; Wang et al., 2024). Our work is most closely aligned with Amber-Pruner (An et al., 2025b), which applies $\{2 : 4, 4 : 8, 8 : 16\}$ semi-structured activation sparsity patterns to already trained models. The authors propose a specific pruning criterion - Amber Pruner and a layer-skipping strategy to avoid sensitive layers. We include Amber Pruner’s criterion in our comparative analysis. While semi-structured **weight**-pruning is well-established for inference efficiency (Han et al., 2015; Frantar & Alistarh, 2023; Kurtić et al., 2023), dynamic activation sparsity remains under-explored despite its theoretical potential (Baykal et al., 2022), and Amber-Pruner (An et al., 2025b) currently is the only paper that explores *post-training sparsification of activations with various sparsity patterns*, which is the primary focus of our work.

Focus and Motivation. Applying N:M sparsity patterns to activations, while conceptually straightforward, raises several key questions: **(Q1) Selection Strategy:** As with weight sparsification, the criterion for selecting which activations to prune is crucial for maintaining performance (Zhelnin et al., 2024). **(Q2) Error Mitigation:** Fine-tuning is a standard method for recovering performance lost to post-training sparsification, but can be prohibitively expensive or risk compromising model safety alignment (Kharinaev et al., 2025). Therefore, we focus on lightweight, *plug-and-play* and *hardware-friendly* approaches that require only minimal calibration data (e.g., WikiText) or no data at all to enhance performance. **(Q3) Beyond 2:4 Patterns:** While **2:4 is the only** hardware-supported semi-structured pattern, we explore a broader range $\{2:4, 4:8, 8:16, 16:32\}$ to motivate future hardware design. While we cannot directly compare acceleration gains between various patterns, our work solely focuses on model performance.

Our Contributions. This paper makes the following key contributions:

- **Activation vs. Weight Sparsity Superiority:** We show that, at similar sparsity levels, activation pruning consistently outperforms weight pruning across four diverse LLMs: Llama2-7B, Llama3-8.1B, Qwen2.5-7B, and Gemma3-4B.
- **Lightweight Error Mitigation and Selection Criteria:** We comprehensively evaluate **four** plug-and-play error mitigation techniques, **three** evaluated for the first time in the context of activation sparsity. We also evaluate **three** pruning selection criteria. These methods include statistical criteria such as median shift and variance correction and provide strong, hardware-friendly baselines for activation sparsification.
- **Exploration of Novel Sparsity Patterns:** We evaluate the performance of sparsity patterns 2:4, 4:8, 8:16, 16:32 . We find that the more flexible 16:32 pattern achieves performance close to unstructured 50% sparsity and is $3\times$ better than 2:4. However, considering hardware implementation, we advocate for the 8:16 pattern, which offers a $2\times$ improvement over 2:4 while remaining highly practical.

2 HARDWARE AND COMPARISON OF 2:4 AND 8:16 SPARSITY

One of the primary aims of our work is to motivate the design of hardware for more flexible sparsity patterns. Currently, only NVIDIA GPUs support structured sparsity, specifically the 2:4 pattern. This pattern achieves 1.5–1.7x inference acceleration and 1.5x energy reduction for 7B models, primarily from a 2x reduction in memory bandwidth (Fang et al., 2024; Lin et al., 2023). At the same time, any N:M pattern beyond 2:4, including 8:16, can provide the same 2x bandwidth reduction but with greater flexibility. In the general $N:M$ format, 2:4 sparsity permits $\binom{4}{2} = 6$ non-zero patterns per block, requiring $\log_2(6)/4 \approx 0.75$ bits per element for metadata. In contrast, the 8:16 pattern allows $\binom{16}{8} = 12,870$ distinct configurations, demanding $\log_2(12,870)/16 \approx 0.875$ bits per element. Stacking four 2:4 blocks to form a 16-element unit yields only $6^4 = 1,296$ configurations—nearly an order of magnitude fewer than the 12,870 offered by a native 8:16 block. Although 8:16 requires slightly more metadata storage, its vastly greater configurational flexibility makes it a compelling candidate. The main trade-off is implementation complexity. Decoding sparsity metadata and gathering non-zero values requires sophisticated circuitry. As the block size M grows, these gather operations could impact performance. However, operating on larger, aligned blocks could also improve cache utilization, potentially amortizing this overhead.

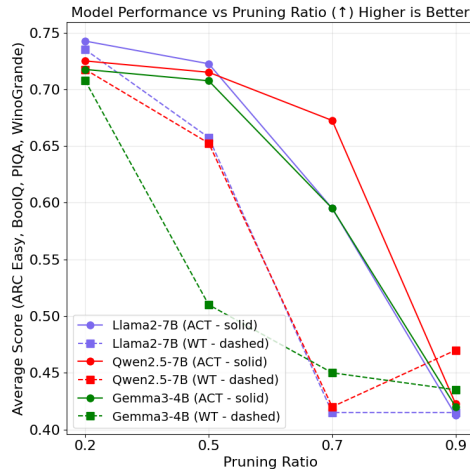


Figure 1: Comparison of **unstructured sparsity** in **activations (ACT)** and **weights (WT)** averaged across four datasets at varying sparsity ratios. **Higher is Better.** More detailed results are presented in Appendix Table 9.

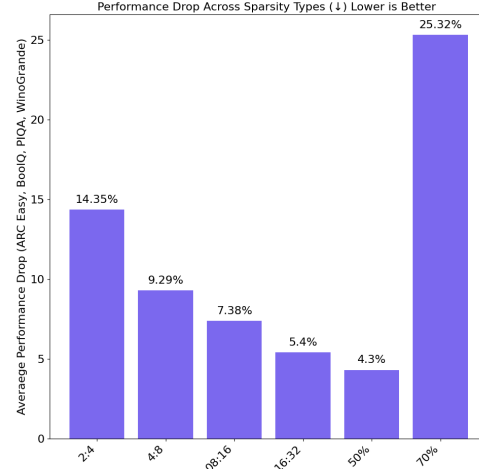


Figure 2: Comparison of sparsity patterns with unstructured sparsity. 50% and 70% correspond to unstructured sparsity. **Lower is Better.** More detailed results are presented in Appendix Table 6.

3 METHODS

3.1 PRELIMINARIES

Consider a linear layer of a LLM with weight \mathbf{W} , input activations \mathbf{X} and output \mathbf{Y} then:

$$\mathbf{Y} = \mathbf{X}\mathbf{W}^\top \quad (1)$$

Our aim is to find a semi-structured pruning mask \mathbf{M} for the activations \mathbf{X} based on some pruning metric S , such that:

$$\mathbf{M}_{ij} = \begin{cases} 1, & S(\mathbf{X}_{ij}) \geq t \\ 0, & S(\mathbf{X}_{ij}) < t \end{cases} \quad (2)$$

where i, j denote the indices of the matrix elements, t is a threshold value chosen to ensure the desired level of sparsity.

Table 1: Briefly describe evaluated activation *pruning metrics* (top) and *transformations* (bottom). Abbreviations in **bold** with an asterisk (*) denote methods proposed here or first evaluated with sparse activations.

Short Name	Method	Key Mechanism
<i>Pruning metrics</i>		
ACT	Magnitude Pruning	Selects based on activation magnitude
WT	Weight-based Pruning	Selects by corresponding weight magnitude
CLACT*	Cosine Loss Activation	A metric inspired by cosine similarity from Mi et al. (2025)
Amber-Pruner (2025a)	Weights Importance	A metric which accounts for important weights after outlier removal and normalization
<i>Transformations</i>		
D-PTS*	Dynamic Per-Token Shift	Batch-wise dynamic centering of activations before sparsification
S-PTS (2024)	Static Per-Token Shift	Fixed centering of activations before sparsification using a per-token bias value pre-collected on WikiText-2
L-PTS*	Learnable Per-Token Shift	Fixed centering of activations before sparsification using per-token bias value learned on WikiText-2
VAR*	Variance Correction	Token-wise variance normalization after sparsification
VAR+L-PTS*	Scaling + Learnable Shift	Apply VAR scaling, then add per-token bias value learned on WikiText-2
R-Sparse (2025)	Rank-Aware Sparsity	Combines sparse activations with weight low-rank SVD factors learned on WikiText-2

Once the mask \mathbf{M} is computed, the output of the linear layer with pruned activations is given by:

$$\mathbf{Y}_p = (\mathbf{X} \odot \mathbf{M}) \mathbf{W}^\top \quad (3)$$

To build **unstructured sparsity**, we apply a global magnitude threshold to every element of the activations (or weights) and zero-out those below the threshold. In **semi-structured 2:4 sparsity**, we split each row (or column) of the matrix into non-overlapping blocks of four consecutive elements; in every block, we keep the two most important entries by a chosen importance metric and set the rest to zero, thereby removing 50% of the elements (Hu et al., 2024). Likewise, we can construct **semi-structured 8:16 sparsity**, achieving the same 50% density but providing greater flexibility with minimal storage overhead (Maximov et al., 2025).

3.2 PRUNING CRITERION

In this study, we primarily consider some pruning metrics. You can find brief descriptions of them in 1.

ACT: This is the magnitude activation pruning metric (**ACT**), defined as the absolute value of the element $\mathbf{X}_{ij} : S_{ACT}(\mathbf{X}_{ij}) = |\mathbf{X}_{ij}|$.

WT: This is the weight-based pruning metric (**WT**), defined as the absolute value of the corresponding weight $\mathbf{W}_{ij} : S_{WT}(\mathbf{W}_{ij}) = |\mathbf{W}_{ij}|$.

CLACT: This metric is inspired by (Mi et al., 2025), which measures the cosine similarity between layer outputs. Building on this concept, we propose a novel metric called Cosine Loss ACTivation (**CLACT**). This approach approximates the cosine distance between an activation \mathbf{X}_{ij} and its feature vector, quantifying each element's importance within its activation row. Unlike magnitude-based methods, CLACT identifies activations that are contextually significant rather than merely large in absolute value.

$$S_{CLACT}(\mathbf{X}_{ij}) = \frac{|\mathbf{X}_{ij}|}{\sqrt{\sum_{k=1}^h \mathbf{X}_{ik}^2}} \sqrt{\sum_{p=1}^l \mathbf{X}_{pj}^2}, \quad (4)$$

where h is hidden dimension, l is sequence length, j is a token number and i an element within this token.

Amber-Pruner: This metric from An et al. (2025b) consists of the following steps: (1) Outlier Removal. To reduce the influence of extreme values, weights \mathbf{W} outside the 0.5th – 99.5th percentiles are discarded: $\mathbf{W} = \{\omega_k \mid Q_{0.005}(\mathbf{W}) \leq \omega_k \leq Q_{0.995}(\mathbf{W})\}$. (2) Normalization. The remaining weights are standardized using their mean and variance: $\hat{\mathbf{W}}_{ij} = (\mathbf{W}_{ij} - \mathbb{E}[\mathbf{W}]) (\text{Var}[\mathbf{W}])^{-\frac{1}{2}}$. (3) Channel-wise Scoring. For each channel $\hat{\mathbf{W}}_{:,j}$, the ℓ_2 norm is computed, and final scores are assigned to activation elements, $\mathcal{L}(\cdot)$ - denotes channel-wise ℓ_2 norm: $S_{\text{Amber-Pruner}}(\mathbf{X}_{ij}) = |\mathbf{X}_{ij}| \cdot \mathcal{L}(\hat{\mathbf{W}}_{:,j})$.

Here, we highlight a critical distinction between CLACT and Amber-Pruner. CLACT is a context aware criterion, particularly useful during the prefill stage since with $l = 1$, it converges to the $L1$ - norm criterion, moreover, it does not consider weight magnitudes. In contrast, Amber-Pruner explicitly prioritizes weights based on their values and remains effective across both prefill and generation stages but does not consider context.

3.3 ERROR MITIGATION AND TRANSFORMATIONS

Since semi-structured pruning of activations can significantly disrupt the outputs of linear layers, additional transformations can be applied to mitigate these negative effects and restore the pruned activations to their original distribution. You can find brief descriptions of them in 1.

PCS: This approach is inspired by SmoothQuant (Xiao et al., 2023) and has been used for 2:4 weight sparsification (Maximov et al., 2025) as well. It uses a per-channel smoothing (**PCS**) factor s applied to activations \mathbf{X} before pruning: $\hat{\mathbf{X}} = \text{diag}(s(\mathbf{X}, \mathbf{W}))^{-1} \mathbf{X}$. To compensate for this transformation, the weight matrix is correspondingly scaled in the opposite direction. As a result, the output of the linear layer is computed as: $\mathbf{Y}_p = (\hat{\mathbf{X}} \odot \mathbf{M})(\text{diag}(s(\mathbf{X}, \mathbf{W}))\mathbf{W}^\top)$. The scale factor s is estimated as Xiao et al. (2023): $s = \sqrt{\max |\mathbf{X}_{:,j}| / (\max |\mathbf{W}_{:,j}^\top|)}$

D-S-L-PTS: The next approach applies a dynamic per-token shift (**D-PTS**) to the input activations \mathbf{X} using a bias term η , such that $\hat{\mathbf{X}} = \mathbf{X} - \eta$. The purpose of this shift is to center most elements of the activations near zero. As a compensatory transformation, the bias η is added to the weights, so the output of the linear layer is given by Chua et al. (2024): $\mathbf{Y}_p = ((\hat{\mathbf{X}} \odot \mathbf{M}) + \eta)\mathbf{W}^\top$, where $\eta = \bar{\mathbf{X}}$. A related variant is the static per-token shift (**S-PTS**), where the bias η is collected during a short warm-up phase and then fixed for all subsequent batches. This reduces computational overhead while providing similar centering effects. Finally, we introduce a learnable per-token shift (**L-PTS**).

VAR: In contrast to the previous approach, this method applies a per-token scaling factor ν to pruned activations such that the output matrix is given as: $\mathbf{Y}_p = \nu(\mathbf{X} \odot \mathbf{M})\mathbf{W}^\top$, The scale factor ν is determined as

$$\nu = \sqrt{\frac{\text{Var}[\mathbf{X}]}{\text{Var}[\mathbf{X} \odot \mathbf{M}]}} \quad (5)$$

We refer to this method as variance correction **VAR**.

VAR+L-PTS: This method is a combination of the per-token scaling with factor **VAR** ν is given by Eq. 5 and the shift **L-PTS**.

R-Sparse: This method from (Kamirul et al., 2025) combines activation sparsity with a low-rank approximation of the weight matrix. We provide more details in Appendix A.

Throughout our experiments we use the WikiText-2 dataset for calibration and learning some parameters. For **S-PTS** we calibrate a single per-channel bias vector η and then keep it fixed for all subsequent batches. For the learnable variant **L-PTS** (and the combined **VAR+L-PTS**) we train η and fine-tune other weights. For **R-Sparse** we train in the same way the low-rank factors of the weight adaptation. In all other methods no parameters are learned or calibrated.

3.4 EVALUATION & MODELS

We begin with a broad funnel of experiments to evaluate all methods listed in Table 1. At this initial stage, we use the **Core Datasets**, Single-Choice and Multi-Choice benchmarks including BoolQ, WinoGrande, PIQA, and ARC-Easy. Once this exploratory phase is complete, we narrow our focus to the most promising approaches, evaluating them primarily on two models: Qwen2.5-7B-Instruct and Llama3-8B-Instruct. This more targeted evaluation phase not only refines the set of methods under consideration but also expands the evaluation to the **Extended Datasets**: HellaSwag, OpenBookQA, RTE, MMLU, Lambada_standard, Lambada_openai, and IFEval. For calibration tasks, when required, we use WikiText-2. This dataset selection follows established model compression practices Egiazarian et al. (2024); Frantar et al. (2022); van Baalen et al. (2024). All evaluations are performed using the LM Eval Harness Gao et al. (2023), and full dataset details are provided in Table 8. **For the models we focus on:** Qwen2.5-7B-Instruct, Llama3-8B-Instruct, Llama2-7B,

Gemma3-4B-Instruct. Importantly, for Qwen2.5-7B-Instruct, we did not sparsify the key, query, or value activations, as preliminary experiments showed severe model degradation when these layers were pruned.

4 RESULTS

4.1 SPARSE WEIGHTS VS. SPARSE ACTIVATIONS

In Figure 1 and Table 9, we demonstrate that unstructured **weight sparsification causes greater model degradation** than unstructured activation sparsification at the same sparsity levels: {20%, 50%, 70%, 90%}. For this evaluation, we specifically use unstructured magnitude-based sparsification, as it is less damaging than semi-structured sparsification and thus provides a lower bound on performance degradation.

4.2 OPTIMAL SEMI-STRUCTURED SPARSITY PATTERNS

Our preliminary investigation demonstrates that while the 16:32 pattern achieves performance close to unstructured sparsity (a 5.4% drop versus 4.5% for 50% unstructured), it requires more metadata and greater resources for gather operations, as discussed in Section 2. Therefore, we focus on the 8:16 pattern, despite its higher performance drop of 7.38%. For comparison, the 2:4 pattern results in a 14.35% drop. These results are shown in Figure 2 and Table 6 in Appendix, we used only magnitude pruning to obtain these results. By demonstrating the superior model quality of 8:16 sparsity, our work incentivizes hardware designers to invest in—or at least consider—supporting the 8:16 pattern.

4.3 EVALUATION OF PRUNING SELECTION CRITERIA ON SINGLE/MULTI-CHOICE DATASETS

We evaluate CLACT, Amber-Pruner, and magnitude pruning as a baseline. The main results for the 2:4 and 8:16 sparsity patterns are presented in Table 2. On average, both CLACT and Amber-Pruner outperform magnitude pruning by at least 2%, however, we observe no clear winner between them. As noted in Section 3.2, these criteria are designed for different purposes: CLACT adjusts based on context, while Amber-Pruner adjusts based on weight magnitudes. Notably, for Llama3-8B under the 2:4 sparsity pattern, simple magnitude pruning outperforms both advanced criteria, underscoring model and architecture-specific sensitivities to pruning strategies.

4.4 EVALUATION OF TRANSFORMATIONS ON SINGLE/MULTI-CHOICE DATASETS

Our main results are presented in Table 2. Surprisingly, we find that simple methods such as dynamic and static per-token shifts (D-PTS, S-PTS) outperform most other approaches. The second most effective methods are VAR and R-SPARSE. We also observe that increasing the number of dimensions in R-SPARSE (from 64 to 128) leads to worse performance, which may indicate overfitting on the calibration data. Finally, we note that L-PTS, the approach with learnable per-token shifts, significantly underperforms compared to its static counterpart, S-PTS.

4.5 EVALUATION TRANSFORMATIONS WITH INSTRUCTION-FOLLOWING TASKS

Table 3 presents instruction-following performance on the IFEval benchmark for Llama3-8B and Qwen2.5-7B, evaluated under two semi-structured sparsity patterns (2:4 and 8:16) and four activation transformation methods: S-PTS, D-PTS, R-Sparse, and VAR. First of all, we observe a strong model degradation on generative tasks. Second of all, we see that VAR is the strongest performer overall, especially for Llama3-8B. S-PTS/D-PTS are competitive and lightweight, and R-Sparse lags significantly, particularly at 2:4. We speculate that while semi-structured patterns are good for prefill stage in LLMs they significantly degrade performance during decode stage. However, as discussed in Section 1 decode stage for single vector can be accelerated with more flexible approaches.

Table 2: Average relative performance (%) across four datasets. Values indicate performance drops (lower is better), negative values signify performance improvement. Methods marked with an asterisk (*) are proposed in this paper. Full, non-aggregated results are available in Appendix 10.

Method	Models				
	Llama2-7B	Qwen2.5-7B	Gemma3-4B	LLama3-8B	Average Drop (↓)
Activations Unstructured 50%					
ACT	2.31%	3.87%	4.80%	4.30%	3.82%
2:4 Weight Sparsity					
WT	16.52%	12.96%	34.86%	33.63%	24.49%
2:4 Activations Selection Criteria					
ACT	9.43%	4.95%	9.94%	14.35%	9.67%
CLACT*	8.32%	-2.45%	8.01%	17.27%	7.79%
Amber-Pruner	11.70%	-1.23%	5.91%	15.01%	7.85%
2:4 Activations Transformations					
VAR*	9.76%	-1.48%	2.96%	13.11%	6.09%
D-PTS*	10.67%	-6.46%	4.58%	14.59%	5.84%
S-PTS	10.37%	-4.43%	3.93%	7.31%	4.29%
L-PTS*	13.13%	3.66%	4.21%	14.13%	8.79%
R-SPARSE (64)	12.90%	-2.55%	5.17%	15.28%	7.70%
R-SPARSE (128)	12.23%	-1.51%	5.16%	16.34%	8.05%
8:16 Weight Sparsity					
WT	7.84%	9.54%	26.11%	27.26%	17.68%
8:16 Activations Selection Criteria					
ACT	5.37%	4.38%	4.76%	7.38%	5.47%
CLACT*	3.98%	-4.02%	0.60%	8.60%	2.29%
Amber-Pruner	5.32%	-6.28%	0.08%	7.13%	1.56%
8:16 Activations Transformations					
VAR*	4.85%	1.93%	-1.87%	8.30%	3.30%
D-PTS*	4.63%	-8.28%	5.16%	6.79%	2.07%
S-PTS	3.87%	-7.24%	-1.54%	7.3 %	0.61%
L-PTS*	8.15%	1.71%	4.21%	7.19%	5.32%
R-SPARSE (64)	5.91%	-6.91%	-1.36%	8.44%	1.52%
R-SPARSE (128)	7.93%	-5.44%	-0.44%	8.44%	2.63%

Table 3: Evaluation with Instruction-Following (IFEval) for Llama3-8B and Qwen2.5-7B. PS denotes prompt-level strict acc, PL denotes prompt-level loose acc.

Model	Original		Pattern	S-PTS		D-PTS		R-Sparse		VAR	
	PS	PL		PS	PL	PS	PL	PS	PL	PS	PL
Llama3-8B	0.4455	0.4861	2:4	0.1682	0.1904	0.1941	0.2015	0.0869	0.0979	0.2237	0.2458
			8:16	0.2995	0.3327	0.2828	0.3198	0.2089	0.2311	0.3161	0.3586
Qwen2.5-7B	0.7135	0.7394	2:4	0.4325	0.5176	0.4399	0.5120	0.2736	0.3457	0.4565	0.5342
			8:16	0.5194	0.5804	0.5434	0.5989	0.3697	0.4196	0.5249	0.5896

Table 4: Performance comparison of pruning methods under 50% and 70% unstructured sparsity for Llama3-8B model.

Model	ARC Easy	BoolQ	PIQA	WinoGrande	Avg. Drop (%)
Original	0.8207	0.8391	0.8003	0.7340	—
Unstructured 50%					
ACT	0.7770	0.8198	0.7714	0.6858	4.45
D-PTS	0.78577	0.8253	0.7807	0.68981	3.60
VAR	0.78409	0.8192	0.77584	0.7048	3.47
CLACT	0.7803	0.8253	0.7655	0.70007	3.89
Amber-Pruner	0.768	0.82018	0.7627	0.7016	4.45
Unstructured 70%					
ACT	0.55808	0.63119	0.6474	0.5477	25.32
D-PTS	0.56481	0.62415	0.6507	0.53433	25.68
VAR	0.61447	0.65107	0.67573	0.5319	22.66
CLACT	0.5551	0.6039	0.62676	0.52407	27.67
Amber-Pruner	0.48737	0.5938	0.5897	0.539	30.68

4.6 SELECTION CRITERIA AND TRANSFORMATIONS FOR UNSTRUCTURED PRUNING

Although unstructured pruning offers limited efficiency gains compared to structured variants, it serves as a valuable proxy task for evaluating the robustness and generalization of proposed methods. We evaluate D-PTS, VAR, and two selection criteria in this experiment: CLACT and Amber-Pruner using the Llama3-8B model. Results in Table 4 indicate that VAR is the most effective transformation under unstructured sparsity. Moreover, CLACT outperforms Amber-Pruner by a wider margin here than in our semi-structured pruning experiments. These findings suggest two key insights: (1) No single method emerges as optimal for both unstructured and semi-structured sparsity. (2) The methods proposed in this work, VAR and CLACT, demonstrate strong generalization and are well-suited for unstructured activation pruning.

4.7 COMBINATION OF TRANSFORMATIONS AND PRUNING CRITERIA

Next, we evaluated combinations of multiple approaches to explore potential performance gains. These combinations and their results are presented in Table 7. As shown, none of the evaluated combinations outperforms any single method, highlighting the challenges of naively combining them.

Table 5: Aggregated results on Llama3-8B with 8:16 activation sparsity with different layers pruned. **ORIG. AVG.** denotes original model performance. **Layers** indicates the subset of linear layers where the method was applied. Non aggregated results are presented in Appendix 12. Drop is computed without accounting for perplexity.

ORIG. AVG.	Method	Layers	PPL	AVG.	Drop ↓
0.6726	LS+L-PTS	all	9.6036	0.6047	10.90%
	LS+L-PTS	key,out,gate,down	8.3483	0.6385	5.43%
	LS+L-PTS	key,value,gate,down	8.0821	0.6503	3.56%
	LS+L-PTS + VAR	all	9.4983	0.6056	10.60%
	LS+L-PTS + VAR	key,out,gate,down	8.2930	0.6422	4.64%
	LS+L-PTS + VAR	key,value,gate,down	8.0259	0.6516	3.36%

4.8 LAYER SENSITIVITY

The next question we investigate in this work is layer sensitivity to activation sparsity. For this experiment, we use the Extended Datasets, the Llama3-8B model, and the 8:16 sparsity pattern. The

main results are presented in Table 5. Here, we focus on methods with learnable parameters, primarily L-PTS and LS (a learnable, diagonal scaling projection). While in most of our experiments, learnable methods underperformed on average compared to static or magnitude-based approaches, the best-performing configurations for Llama3-8B under 8:16 sparsity were, in fact, those employing learnable parameters — as shown in Table 5. We find that activations from the up projection (in the FFN) and the out projection¹ are the most sensitive to sparsification, pruning these layers leads to the most significant performance drops, suggesting they should be preserved or treated with greater care in compression strategies. While we can not say this generalizes across all layers, we empirically demonstrate that some layers are more important than others.

5 DISCUSSION

The performance gap between multiple/single-choice benchmarks (e.g., BoolQ, PIQA) and IFEval likely stems from differences in the inference stages they emphasize. Core QA benchmarks primarily stress the prefill phase, whereas IFEval evaluates both prefill and autoregressive generation. Our evaluation remains valid: semi-structured patterns like 2:4 and 8:16 are especially effective at accelerating the prefill stage, which often dominates inference latency.

6 LIMITATIONS

Our work has three main limitations. First, evaluations rely on software emulation, precluding real-world measurements of speedup or energy savings on hardware supporting sparsity beyond 2:4. Second, our layer sensitivity analysis is preliminary, while up-projection and out-projection layers appear most vulnerable, broader architectural studies are needed. Third, Qwen2.5-7B shows anomalous gains on multiple-choice benchmarks under certain sparsification methods, an artifact we attribute to benchmark limitations, as no such gains appear on IFEval. Critically, generative performance degrades significantly, underscoring the need for evaluation beyond multiple-choice QA.

7 CONCLUSION

This work establishes that post-training activation pruning is more accuracy preserving than weight pruning for Large Language Models. Across four diverse LLMs, we demonstrate that activation pruning consistently preserves a model’s capabilities better than weight pruning at equivalent sparsity levels, highlighting its potential for dynamic, input-adaptive efficiency gains.

Our key novel contributions are twofold. First, we conduct the first comprehensive evaluation of lightweight, plug-and-play error mitigation techniques for activation sparsity, including the introduction and evaluation of three new methods: Cosine Loss Activation (CLACT) as a context-aware pruning criterion, Dynamic/Learnable Per-Token Shift (D-PTS/L-PTS) and Variance Correction (VAR). We show that these simple methods, often outperforming more complex approaches, providing strong, hardware-friendly baselines for the community. Second, we systematically explore semi-structured sparsity patterns beyond the hardware standard 2:4. We find that the 8:16 pattern offers more flexibility and, ultimately, lower model degradation. Although the 16:32 pattern performs even closer to unstructured sparsity, we advocate for 8:16 as the optimal target for future hardware design due to its balance of performance gain and implementation feasibility. In summary, this work not only provides practical, high-performing methods for post-training activation pruning but also creates grounded motivation for 8:16 structured sparsity support, which would unlock significant efficiency gains for LLM inference with minimal added complexity.

Acknowledgment on LLM assisted writing: This paper used open access Qwen3-Max, in some parts of the paper, for proofreading and text rephrasing in accordance with formal style.

¹The output projection of the attention mechanism. It combines outputs from all attention heads and projects them back to the model’s hidden dimension.

REFERENCES

Tai An, Ruwu Cai, Yanzhe Zhang, Yang Liu, Hao Chen, Pengcheng Xie, Sheng Chang, Yiwu Yao, and Gongyi Wang. Amber pruner: Leveraging n: M activation sparsity for efficient prefill in large language models. *arXiv preprint arXiv:2508.02128*, 2025a.

Tai An, Ruwu Cai, Yanzhe Zhang, Yang Liu, Hao Chen, Pengcheng Xie, Sheng Chang, Yiwu Yao, and Gongyi Wang. Amber pruner: Leveraging n:m activation sparsity for efficient prefill in large language models, 2025b. URL <https://arxiv.org/abs/2508.02128>.

Roy Bar-Haim, Ido Dagan, Bill Dolan, Lisa Ferro, Danilo Giampiccolo, Bernardo Magnini, and Idan Szpektor. The second pascal recognising textual entailment challenge. In *Proceedings of the Second PASCAL Challenges Workshop*, 2006.

Cenk Baykal, Nishanth Dikkala, Rina Panigrahy, Cyrus Rashtchian, and Xin Wang. A theoretical view on sparsely activated networks. *Advances in Neural Information Processing Systems*, 35: 30071–30084, 2022.

Yonatan Bisk, Rowan Zellers, Jianfeng Gao, and Yejin Choi. Piqa: Reasoning about physical commonsense in natural language. In *Proceedings of AAAI*, 2020.

Vui Seng Chua, Yujie Pan, and Nilesh Jain. Post-training statistical calibration for higher activation sparsity. *arXiv preprint arXiv:2412.07174*, 2024.

Christopher Clark, Kenton Lee, Ming-Wei Chang, Tom Kwiatkowski, Michael Collins, and Kristina Toutanova. Boolq: Exploring the surprising difficulty of natural yes/no questions. In *Proceedings of NAACL-HLT*, pp. 2924–2936, 2019.

Peter Clark, Isaac Cowhey, Oren Etzioni, Tushar Khot, Ashish Sabharwal, Carissa Schoenick, and Oyvind Tafjord. Think you have solved question answering? try arc, the ai2 reasoning challenge. *arXiv:1803.05457v1*, 2018.

Karl Cobbe, Vineet Kosaraju, Mohammad Bavarian, Mark Chen, Heewoo Jun, Lukasz Kaiser, Matthias Plappert, Jerry Tworek, Jacob Hilton, Reiichiro Nakano, Christopher Hesse, and John Schulman. Training verifiers to solve math word problems. *arXiv preprint arXiv:2110.14168*, 2021.

Ido Dagan, Oren Glickman, and Bernardo Magnini. The pascal recognising textual entailment challenge. In *Machine Learning Challenges Workshop*, pp. 177–190. Springer, 2005.

Vage Egiazarian, Andrei Panferov, Denis Kuznedelev, Elias Frantar, Artem Babenko, and Dan Alistarh. Extreme compression of large language models via additive quantization. *arXiv preprint arXiv:2401.06118*, 2024.

Ege Erdil. Inference economics of language models. *arXiv preprint arXiv:2506.04645*, 2025.

Gongfan Fang, Hongxu Yin, Saurav Muralidharan, Greg Heinrich, Jeff Pool, Jan Kautz, Pavlo Molchanov, and Xinchao Wang. Maskllm: Learnable semi-structured sparsity for large language models. *Advances in Neural Information Processing Systems*, 37:7736–7758, 2024.

Elias Frantar and Dan Alistarh. Sparsegpt: Massive language models can be accurately pruned in one-shot. In *International conference on machine learning*, pp. 10323–10337. PMLR, 2023.

Elias Frantar, Saleh Ashkboos, Torsten Hoefler, and Dan Alistarh. Gptq: Accurate post-training quantization for generative pre-trained transformers. *arXiv preprint arXiv:2210.17323*, 2022.

Leo Gao, Jonathan Tow, Baber Abbasi, Stella Biderman, Sid Black, Anthony DiPofi, Charles Foster, Laurence Golding, Jeffrey Hsu, Alain Le Noac'h, Haonan Li, Kyle McDonell, Niklas Muenighoff, Chris Ociepa, Jason Phang, Laria Reynolds, Hailey Schoelkopf, Aviya Skowron, Lin-tang Sutawika, Eric Tang, Anish Thite, Ben Wang, Kevin Wang, and Andy Zou. A framework for few-shot language model evaluation, 12 2023. URL <https://zenodo.org/records/10256836>.

Song Han, Jeff Pool, John Tran, and William J. Dally. Learning both weights and connections for efficient neural networks, 2015. URL <https://arxiv.org/abs/1506.02626>.

Daniel Haziza, Timothy Chou, Dhruv Choudhary, Luca Wehrstedt, Francisco Massa, Jiecao Yu, Geonhwa Jeong, Supriya Rao, Patrick Labatut, and Jesse Cai. Accelerating transformer inference and training with 2: 4 activation sparsity. *arXiv preprint arXiv:2503.16672*, 2025.

Dan Hendrycks, Collin Burns, Steven Basart, Andy Zou, Mantas Mazeika, Dawn Song, and Jacob Steinhardt. Measuring massive multitask language understanding. *arXiv preprint arXiv:2009.03300*, 2020.

Yuezhou Hu, Kang Zhao, Weiyu Huang, Jianfei Chen, and Jun Zhu. Accelerating transformer pre-training with 2: 4 sparsity. *arXiv preprint arXiv:2404.01847*, 2024.

Itay Hubara, Brian Chmiel, Moshe Island, Ron Banner, Joseph Naor, and Daniel Soudry. Accelerated sparse neural training: A provable and efficient method to find $n: m$ transposable masks. *Advances in neural information processing systems*, 34:21099–21111, 2021.

Kamirul Kamirul, Odysseas Pappas, and Alin Achim. R-sparse r-cnn: Sar ship detection based on background-aware sparse learnable proposals, 2025. URL <https://arxiv.org/abs/2504.18959>.

Artyom Kharinaev, Viktor Moskvoretskii, Egor Shvetsov, Kseniia Studenikina, Bykov Mikhail, and Evgeny Burnaev. Investigating the impact of quantization methods on the safety and reliability of large language models. *arXiv preprint arXiv:2502.15799*, 2025.

Eldar Kurtić, Elias Frantar, and Dan Alistarh. Ziplm: Inference-aware structured pruning of language models. *Advances in Neural Information Processing Systems*, 36:65597–65617, 2023.

Je-Yong Lee, Donghyun Lee, Genghan Zhang, Mo Tiwari, and Azalia Mirhoseini. Cats: Contextually-aware thresholding for sparsity in large language models, 2024. URL <https://arxiv.org/abs/2404.08763>, 2024.

Bin Lin, Ningxin Zheng, Lei Wang, Shijie Cao, Lingxiao Ma, Quanlu Zhang, Yi Zhu, Ting Cao, Jilong Xue, Yuqing Yang, et al. Efficient gpu kernels for $n: M$ -sparse weights in deep learning. *Proceedings of Machine Learning and Systems*, 5:513–525, 2023.

James Liu, Pragaash Ponnusamy, Tianle Cai, Han Guo, Yoon Kim, and Ben Athiwaratkun. Training-free activation sparsity in large language models. *arXiv preprint arXiv:2408.14690*, 2024.

Zhuang Liu, Jianguo Li, Zhiqiang Shen, Gao Huang, Shoumeng Yan, and Changshui Zhang. Learning efficient convolutional networks through network slimming. In *Proceedings of the IEEE international conference on computer vision*, pp. 2736–2744, 2017.

Zichang Liu, Jue Wang, Tri Dao, Tianyi Zhou, Binhang Yuan, Zhao Song, Anshumali Shrivastava, Ce Zhang, Yuandong Tian, Christopher Re, et al. Deja vu: Contextual sparsity for efficient llms at inference time. In *International Conference on Machine Learning*, pp. 22137–22176. PMLR, 2023.

Egor Maximov, Yulia Kuzkina, Azamat Kanametov, Alexander Prutko, Aleksei Goncharov, Maxim Zhelnin, and Egor Shvetsov. From 2: 4 to 8: 16 sparsity patterns in llms for outliers and weights with variance correction. *arXiv preprint arXiv:2507.03052*, 2025.

Stephen Merity, Caiming Xiong, James Bradbury, and Richard Socher. Pointer sentinel mixture models, 2016.

Zhendong Mi, Zhenglun Kong, Geng Yuan, and Shaoyi Huang. Ace: Exploring activation cosine similarity and variance for accurate and calibration-efficient llm pruning. *arXiv preprint arXiv:2505.21987*, 2025.

Todor Mihaylov, Peter Clark, Tushar Khot, and Ashish Sabharwal. Can a suit of armor conduct electricity? a new dataset for open book question answering. In *Proceedings of EMNLP*, pp. 2381–2391, 2018.

Iman Mirzadeh, Keivan Alizadeh, Sachin Mehta, Carlo C Del Mundo, Oncel Tuzel, Golnoosh Samei, Mohammad Rastegari, and Mehrdad Farajtabar. Relu strikes back: Exploiting activation sparsity in large language models. *arXiv preprint arXiv:2310.04564*, 2023.

Pavlo Molchanov, Arun Mallya, Stephen Tyree, Iuri Frosio, and Jan Kautz. Importance estimation for neural network pruning. In *Proceedings of the IEEE/CVF conference on computer vision and pattern recognition*, pp. 11264–11272, 2019.

Denis Paperno, Germán Kruszewski, Angeliki Lazaridou, Quan Ngoc Pham, Raffaella Bernardi, Sandro Pezzelle, Marco Baroni, Gemma Boleda, and Raquel Fernández. The lambada dataset: Word prediction requiring a broad discourse context. *arXiv preprint arXiv:1606.06031*, 2016.

Mansheej Paul, Feng Chen, Brett W Larsen, Jonathan Frankle, Surya Ganguli, and Gintare Karolina Dziugaite. Unmasking the lottery ticket hypothesis: What’s encoded in a winning ticket’s mask? *arXiv preprint arXiv:2210.03044*, 2022.

Keisuke Sakaguchi, Rowan Zellers, Ari Holtzman, and Yejin Choi. Winogrande: An adversarial winograd schema challenge at scale. In *Proceedings of AAAI*, 2020.

Susav Shrestha, Brad Settlemeyer, Nikoli Dryden, and Narasimha Reddy. Polar sparsity: High throughput batched llm inferencing with scalable contextual sparsity. *arXiv preprint arXiv:2505.14884*, 2025.

Egor Shvetsov, Dmitry Osin, Alexey Zaytsev, Ivan Koryakovskiy, Valentin Buchnev, Ilya Trofimov, and Evgeny Burnaev. Quantnas for super resolution: Searching for efficient quantization-friendly architectures against quantization noise. *IEEE Access*, 12:117008–117025, 2024. doi: 10.1109/ACCESS.2024.3446039.

Yixin Song, Zeyu Mi, Haotong Xie, and Haibo Chen. Powerinfer: Fast large language model serving with a consumer-grade gpu. In *Proceedings of the ACM SIGOPS 30th Symposium on Operating Systems Principles*, pp. 590–606, 2024a.

Yixin Song, Haotong Xie, Zhengyan Zhang, Bo Wen, Li Ma, Zeyu Mi, and Haibo Chen. Turbo sparse: Achieving llm sota performance with minimal activated parameters. *arXiv preprint arXiv:2406.05955*, 2024b.

Mart van Baalen, Andrey Kuzmin, Markus Nagel, Peter Couperus, Cedric Bastoul, Eric Mahurin, Tijmen Blankevoort, and Paul Whatmough. Gptvq: The blessing of dimensionality for llm quantization. *arXiv preprint arXiv:2402.15319*, 2024.

Hongyu Wang, Shuming Ma, Ruiping Wang, and Furu Wei. Q-sparse: All large language models can be fully sparsely-activated. *arXiv preprint arXiv:2407.10969*, 2024.

Guangxuan Xiao, Ji Lin, Mickael Seznec, Hao Wu, Julien Demouth, and Song Han. Smoothquant: Accurate and efficient post-training quantization for large language models. In *International Conference on Machine Learning*, pp. 38087–38099. PMLR, 2023.

Rowan Zellers, Ari Holtzman, Yonatan Bisk, Ali Farhadi, and Yejin Choi. Hellaswag: Can a machine really finish your sentence? In *Proceedings of ACL*, 2019.

Maxim Zhelnin, Viktor Moskvoretskii, Egor Shvetsov, Egor Venediktov, Mariya Krylova, Aleksandr Zuev, and Evgeny Burnaev. Gift-sw: Gaussian noise injected fine-tuning of salient weights for llms. *arXiv preprint arXiv:2408.15300*, 2024.

Jeffrey Zhou, Tianjian Lu, Swaroop Mishra, Siddhartha Brahma, Sujoy Basu, Yi Luan, Denny Zhou, and Le Hou. Instruction-following evaluation for large language models, 2023. URL <https://arxiv.org/abs/2311.07911>.

Chenzhuo Zhu, Song Han, Huizi Mao, and William J Dally. Trained ternary quantization. *arXiv preprint arXiv:1612.01064*, 2016.

APPENDIX

A R-SPARSE DETAILS

Finally, we include **R-Sparse** (Kamirul et al., 2025), which combines activation sparsity with a low-rank approximation of the weight matrix. Instead of pruning solely by magnitude, R-Sparse decomposes the computation into two parts: (i) sparse channels with high-magnitude activations, and (ii) a low-rank component obtained via SVD of \mathbf{W} that approximates the contribution of pruned activations.

Formally, the linear layer

$$\mathbf{Y} = \mathbf{X}\mathbf{W}^\top \quad (6)$$

is approximated as

$$\mathbf{Y} \approx \mathbf{Y}_s + \mathbf{Y}_r, \quad (7)$$

where

$$\mathbf{Y}_s = \sigma_{t(s)}(\mathbf{X})\mathbf{W}^\top, \quad \mathbf{Y}_r = (\mathbf{X} - \sigma_{t(s)}(\mathbf{X}))(A_r B_r)^\top. \quad (8)$$

Here $\sigma_{t(s)}(\cdot)$ denotes sparsification of activations with threshold $t(s)$, and $A_r B_r^\top$ is the rank- r approximation of \mathbf{W} obtained from its truncated SVD. The trade-off between \mathbf{Y}_s and \mathbf{Y}_r is determined by a sparsity budget s and rank r , which can be optimized via evolutionary search.

B DIFFERENT PATTERNS FOR SEMI-STRUCTURE SPARSIFICATION

Table 6: Performance comparison of different sparsity patterns on Llama3-8B across various benchmarks. Values represent accuracy scores, with the last column showing the average performance drop relative to the original model.

	ARC Easy	BoolQ	PIQA	WinoGrande	Avg Drop (\downarrow)
Original	0.8207	0.8391	0.8003	0.7340	
2:4	0.6837	0.7261	0.7163	0.6110	14.35%
4:8	0.7272	0.7810	0.7529	0.6393	9.29%
8:16	0.7525	0.7969	0.7568	0.6551	7.38%
16:32	0.7698	0.8082	0.7688	0.6771	5.40%
50% unstructured	0.7820	0.8198	0.7714	0.6858	4.30%
70% unstructured	0.5580	0.6311	0.6474	0.5477	25.32%

B.1 COMPARISON OF DIFFERENT PATTERNS

Table 7: **A comparison of combined approaches with 8:16 semi-structured sparsity.** Average relative performance (%) across four datasets. Values indicate performance drops (lower is better), negative values signify performance improvement. Full, non-aggregated results are available in Appendix 10.

Method	Models				Average Drop (\downarrow)
	Llama2-7B	Qwen2.5-7B	Gemma3-4B	LLama3-8B	
CLACT + PTS	5.63%	-5.06%	0.50%	8.55%	2.40%
CLACT + VAR	5.07%	-2.90%	0.54%	8.59%	2.82%
Amber-Pruner + PTS	6.16%	-3.47%	0.17%	7.42%	2.57%
Amber-Pruner + VAR	4.74%	-3.63%	-0.16%	8.39%	2.34%
L-PTS + VAR	6.87%	2.86%	3.41%	7.15%	5.07%

C DATASETS

Table 8: Datasets used to evaluate hypotheses. *Prompt-level strict accuracy* is the fraction of prompts for which all verifiable instructions in the prompt are followed exactly as stated. *Instruction-level strict accuracy* is the fraction of individual instructions that are followed exactly as stated, averaged across all instructions.

Dataset	Description	Metric
WikiText-2 (Merity et al., 2016)	A collection of over 100 million tokens extracted from the set of verified Good and Featured articles on Wikipedia.	Perplexity
ARC-Easy (Clark et al., 2018)	QA benchmark for genuine grade-school level, multiple-choice science questions. The dataset contains 2251 examples for training, 570 for development and 2376 for testing.	Accuracy
ARC_Challenge (Clark et al., 2018)	QA benchmark for more difficult grade-school level science questions, part of the AI2 Reasoning Challenge. Designed to require deeper reasoning than ARC-Easy.	Accuracy
BoolQ (Clark et al., 2019)	QA benchmark for yes/no questions. The dataset contains 9427 examples for training and 3270 for testing.	Accuracy
PIQA (Bisk et al., 2020)	Physical commonsense QA benchmark for choosing the right answer between two options. Contains 16K train, 2K dev, and 3K test examples.	Accuracy
WinoGrande (Sakaguchi et al., 2020)	QA benchmark for pronoun resolution with adversarial filtering. Contains 40K train, 1267 dev, and 1767 test examples.	Accuracy
HellaSwag (Zellers et al., 2019)	Commonsense reasoning benchmark for sentence completion, designed to be easy for humans but hard for models. Contains 70K train and 10K validation examples.	Accuracy
OpenBookQA (Mihaylov et al., 2018)	Open-book question answering dataset requiring retrieval of elementary science facts. Contains 5957 4-way multiple-choice questions.	Accuracy
RTE (Dagan et al., 2005; Bar-Haim et al., 2006)	Recognizing Textual Entailment datasets from PASCAL challenges. Task is to classify if a hypothesis is entailed by a premise.	Accuracy
MMLU (Hendrycks et al., 2020)	Massive Multitask Language Understanding benchmark covering 57 subjects across STEM, humanities, and social sciences. Measures multitask accuracy.	Accuracy
Lambada_Standard (Paperno et al., 2016)	Word prediction task requiring broad discourse context. Target word is unpredictable from local context alone.	Accuracy
Lambada_OpenAI (Paperno et al., 2016)	LAMBADA test set preprocessed by OpenAI for standardized evaluation. Task remains final word prediction with long-range dependencies.	Accuracy
GSM8K (Cobbe et al., 2021)	Grade school math word problems requiring multi-step reasoning. Contains 7.5K train and 1.3K test examples.	Accuracy (Strict) Accuracy (Flexible)
IFEval (Zhou et al., 2023)	Benchmark with 541 prompts containing verifiable instructions to measure instruction-following fidelity.	Accuracy (Prompt-level) Accuracy (Instruct-level)

D WEIGHTS VERSUS ACTIVATIONS

Table 9: The performance of models with applied unstructured activation pruning. We show that even with severe sparsity (70-90%) models were able to perform decently on our benchmarks. **ACT** stands for activations pruning, **WT** — for weight pruning. **OUT** denotes values more than 2^3 , according accuracy scores most likely correspond to random.

Pruning	WikiText2 ↓	ARC Easy	BoolQ	PIQA	WinoGrande	Drop (↓)%
Llama2-7B						
Base	6.94	0.74	0.80	0.76	0.66	-
0.2 ACT	6.96	0.74	0.80	0.77	0.66	-0.33%
0.2 WT	7.49	0.72	0.80	0.76	0.66	0.68%
0.5 ACT	7.53	0.70	0.78	0.75	0.66	2.32%
0.5 WT	18.72	0.60	0.72	0.70	0.61	11.10%
0.7 ACT	20.11	0.56	0.64	0.65	0.53	19.62%
0.7 WT	OUT	0.27	0.38	0.54	0.47	43.44%
0.9 ACT	OUT	0.26	0.38	0.52	0.49	43.39%
0.9 WT	OUT	0.27	0.38	0.53	0.48	43.39%
Qwen2.5-7B						
Base	7.46	0.69	0.86	0.75	0.60	-
0.2 ACT	7.48	0.69	0.86	0.74	0.61	2.37%
0.2 WT	8.03	0.67	0.86	0.74	0.60	3.42%
0.5 ACT	8.3	0.67	0.87	0.74	0.58	3.87%
0.5 WT	43.6	0.56	0.80	0.68	0.57	3.42%
0.7 ACT	18.7	0.6	0.81	0.70	0.58	3.87%
0.7 WT	OUT	0.28	0.38	0.54	0.48	12.12%
0.9 ACT	OUT	0.25	0.38	0.54	0.52	44.22%
0.9 WT	OUT	0.25	0.58	0.54	0.51	36.35%
Gemma3-4B						
Base	17.29	0.72	0.84	0.72	0.62	-
0.2 ACT	17.60	0.71	0.84	0.72	0.60	3.35%
0.2 WT	18.93	0.68	0.84	0.72	0.59	4.74%
0.5 ACT	22.39	0.71	0.83	0.72	0.57	4.80%
0.5 WT	273	0.36	0.55	0.61	0.52	30.89%
0.7 ACT	88	0.55	0.63	0.66	0.54	19.57%
0.7 WT	OUT	0.27	0.49	0.53	0.51	38.81%
0.9 ACT	OUT	0.26	0.38	0.54	0.50	42.64%
0.9 WT	OUT	0.25	0.45	0.52	0.52	40.60%

E MAIN EXTENDED RESULTS

In this section we present non - aggregated results for all of the methods and datasets., results are presented in Table 11 and Table 10.

Table 10: **Semi-Structured 2:4 Sparsification** - performance Metrics, for calibration, when it is required, and perplexity we use WikiText2. Average Drop is computed without accounting for perplexity

Pruning	WikiText2 ↓	ARC Easy	BoolQ	PIQA	WinoGrande	Average Drop %
Llama2-7B	6.94	0.74	0.80	0.76	0.66	-
ACT	10.23	0.66	0.71	0.71	0.60	9.43%
WT	42.40	0.57	0.65	0.69	0.56	16.52%
D-PTS	9.38	0.64	0.68	0.71	0.61	10.67%
S-PTS	9.36	0.66	0.68	0.71	0.60	10.37%
VAR	8.31	0.67	0.69	0.72	0.59	9.76%
CLACT	8.23	0.65	0.72	0.71	0.63	8.32%
Amber-Pruner	9.24	0.64	0.68	0.69	0.60	11.70%
LPTS	8.89	0.65	0.60	0.72	0.59	13.13%
LPTS + VAR	8.39	0.67	0.63	0.72	0.60	11.47%
R-SPARSE (64)	9.19	0.66	0.63	0.69	0.59	12.90%
R-SPARSE (128)	9.29	0.65	0.65	0.70	0.59	12.23%
Llama3.1-8B	7.21	0.82	0.84	0.80	0.73	-
ACT	16.61	0.68	0.73	0.72	0.61	14.35%
WT	20.14	0.41	0.57	0.60	0.54	33.63%
PTS	16.4	0.69	0.73	0.72	0.60	14.59%
S-PTS (N-100)	16.5	0.67	0.74	0.72	0.60	14.61%
S-PTS (N-200)	16.5	0.68	0.73	0.72	0.61	14.31%
VAR	14.17	0.70	0.73	0.73	0.62	13.11%
CLACT	19.49	0.65	0.71	0.69	0.59	17.27%
WANDA	15.86	0.66	0.74	0.69	0.61	15.01%
L-PTS	12.77	0.71	0.71	0.73	0.59	14.13%
L-PTS + VAR	12.40	0.73	0.71	0.73	0.60	13.49%
R-SPARSE (64)	15.07	0.69	0.72	0.71	0.61	15.28%
R-SPARSE (128)	16.09	0.67	0.71	0.70	0.61	16.34%
Qwen2.5-7B	7.46	0.69	0.86	0.75	0.60	-
ACT	10.06	0.65	0.86	0.72	0.54	4.95%
WT	35.37	0.53	0.78	0.68	0.54	12.96%
D-PTS	10.07	0.79	0.86	0.76	0.66	-6.46%
S-PTS	10.74	0.78	0.84	0.74	0.65	-4.43%
VAR	13.95	0.74	0.83	0.74	0.61	-1.48%
CLACT	11.16	0.73	0.84	0.71	0.67	-2.45%
Amber-Pruner	10.64	0.74	0.84	0.70	0.64	-1.23%
LPTS	9.13	0.67	0.81	0.72	0.58	3.66%
LPTS + VAR	9.10	0.68	0.81	0.73	0.56	3.97%
R-SPARSE (64)	9.03	0.79	0.76	0.75	0.64	-2.55%
R-SPARSE (128)	9.12	0.77	0.77	0.75	0.63	-1.51%
Gemma3-4B	17.29	0.72	0.84	0.72	0.62	-
ACT	35.62	0.65	0.76	0.70	0.51	9.94%
WT	421.95	0.35	0.44	0.58	0.49	34.86%
D-PTS	35.94	0.70	0.76	0.70	0.60	4.58%
S-PTS	35.84	0.71	0.77	0.70	0.60	3.93%
VAR	33.25	0.60	0.76	0.63	0.54	5.04%
CLACT	39.22	0.66	0.74	0.67	0.59	8.01%
Amber-Pruner	35.56	0.67	0.76	0.68	0.61	5.91%
LPTS	19.55	0.65	0.73	0.70	0.55	9.19%
LPTS + VAR	19.13	0.65	0.74	0.71	0.53	9.82%
R-SPARSE (64)	17.04	0.69	0.76	0.69	0.60	5.17%
R-SPARSE (128)	16.17	0.68	0.75	0.70	0.61	5.16%

Table 11: **Semi-Structured 8:16 Sparsification** - performance Metrics, for calibration, when it is required, and perplexity we use WikiText2. Average Drop is computed without accounting for perplexity.

Pruning	WikiText2 ↓	ARC Easy	BoolQ	PIQA	WinoGrande	Average Drop %
Llama2-7B	6.94	0.74	0.80	0.76	0.66	-
ACT	8.12	0.69	0.75	0.73	0.63	5.37%
WT	20.47	0.64	0.76	0.72	0.61	7.84%
D-PTS	6.92	0.70	0.73	0.75	0.64	4.63%
S-PTS	6.93	0.70	0.73	0.75	0.66	3.87%
VAR	6.67	0.69	0.72	0.75	0.65	4.85%
CLACT	6.54	0.71	0.74	0.75	0.64	3.98%
CLACT + PTS	7.00	0.69	0.72	0.73	0.64	5.63%
CLACT + VAR	6.72	0.69	0.73	0.75	0.64	5.07%
R-SPARSE (64)	7.75	0.69	0.71	0.73	0.64	5.91%
R-SPARSE (128)	7.82	0.68	0.69	0.74	0.61	7.93%
Amber-Pruner	8.10	0.66	0.75	0.73	0.66	5.32%
Amber-Pruner + PTS	6.90	0.68	0.72	0.72	0.65	6.16%
Amber-Pruner + VAR	6.66	0.70	0.72	0.74	0.65	4.74%
LPTS	7.50	0.69	0.66	0.74	0.63	8.15%
LPTS + VAR	7.52	0.69	0.67	0.74	0.64	6.87%
Llama3.1-8B	7.21	0.82	0.84	0.80	0.73	-
ACT	10.32	0.75	0.80	0.76	0.66	7.38%
WT	22.56	0.51	0.64	0.63	0.54	27.26%
D-PTS	10.34	0.76	0.80	0.76	0.66	6.79%
S-PTS	10.31	0.76	0.80	0.75	0.66	7.30%
VAR	10.67	0.74	0.79	0.75	0.66	8.30%
CLACT	10.67	0.73	0.79	0.74	0.66	8.60%
CLACT + PTS	10.68	0.74	0.79	0.74	0.65	8.55%
CLACT + VAR	10.15	0.74	0.79	0.75	0.64	8.59%
R-SPARSE (64)	11.42	0.75	0.77	0.75	0.66	8.44%
R-SPARSE (128)	10.43	0.75	0.78	0.74	0.66	8.49%
Amber-Pruner	10.16	0.73	0.80	0.75	0.68	7.13%
Amber-Pruner + PTS	10.17	0.75	0.80	0.75	0.66	7.42%
Amber-Pruner + VAR	9.94	0.74	0.80	0.75	0.64	8.39%
LPTS	10.04	0.76	0.79	0.77	0.65	7.19%
LPTS + VAR	10.26	0.77	0.78	0.76	0.66	7.15%
Qwen2.5-7B	7.46	0.69	0.86	0.75	0.60	-
ACT	8.61	0.66	0.87	0.73	0.53	4.38%
WT	40.79	0.59	0.82	0.67	0.52	9.54%
D-PTS	8.61	0.80	0.87	0.77	0.68	-8.28%
S-PTS	8.84	0.80	0.86	0.76	0.67	-7.24%
VAR	11.91	0.69	0.72	0.75	0.65	1.93%
CLACT	8.94	0.77	0.85	0.73	0.65	-4.02%
CLACT + PTS	8.94	0.77	0.86	0.83	0.67	-5.06%
CLACT + VAR	8.87	0.76	0.84	0.71	0.65	-2.90%
R-SPARSE (64)	8.12	0.82	0.79	0.77	0.69	-6.90%
R-SPARSE (128)	8.24	0.80	0.79	0.77	0.67	-5.40%
Amber-Pruner	8.80	0.77	0.86	0.74	0.69	-6.20%
Amber-Pruner + PTS	8.79	0.77	0.85	0.73	0.64	-3.40%
Amber-Pruner + VAR	8.73	0.75	0.85	0.74	0.65	-3.60%
LPTS	8.23	0.69	0.83	0.75	0.57	1.70%
LPTS + VAR	8.21	0.70	0.83	0.73	0.56	2.80%
Gemma3-4B	17.29	0.72	0.84	0.72	0.62	-
ACT	25.31	0.70	0.81	0.71	0.55	4.76%
WT	198.53	0.39	0.60	0.62	0.52	26.11%
D-PTS	25.17	0.70	0.81	0.71	0.54	5.16%
S-PTS	25.40	0.75	0.82	0.74	0.63	-1.54%
VAR	23.93	0.75	0.81	0.73	0.65	-1.87%
CLACT	25.85	0.75	0.81	0.71	0.61	0.60%
CLACT + PTS	26.03	0.73	0.81	0.70	0.63	0.50%
CLACT + VAR	24.78	0.74	0.81	0.70	0.63	0.54%
R-SPARSE (64)	15.39	0.76	0.80	0.74	0.64	-1.36%
R-SPARSE (128)	14.55	0.74	0.80	0.73	0.63	-0.44%
Amber-Pruner	25.11	0.74	0.82	0.70	0.63	0.08%
Amber-Pruner + PTS	25.28	0.75	0.81	0.70	0.63	0.17%
Amber-Pruner + VAR	23.97	0.74	0.81	0.71	0.64	-0.16%
LPTS	15.73	0.70	0.79	0.73	0.56	4.21%
LPTS + VAR	15.68	0.71	0.79	0.72	0.57	3.41%

Table 12: Llama3-8B with 8:16 activation sparsity. LS+L-PTS indicates Learnable Diagonal Scale + Learnable Shift, “Layers” indicates the subset of linear layers where the method was applied. Drop is computed without accounting for perplexity.

Method	Layers	PPL	BoolQ	WinoGrande	PIQA	ARC Easy	ARC Chall.	HellaSwag	OpenBookQA	RTE	MMLU	Lambada stand.	Lambada (OpenAI)	Drop % ↓
ORIGINAL	—	—	0.8391	0.7340	0.8003	0.8207	0.5196	0.5905	0.3420	0.6859	0.6790	0.6569	0.7308	—
LS+L-PTS	all	9.6036	0.7841	0.6638	0.7715	0.7647	0.4514	0.5294	0.2720	0.6318	0.5521	0.5686	0.6625	10.90%
LS+L-PTS	k.o.gate.down	8.3483	0.8205	0.7111	0.7889	0.7887	0.4659	0.5591	0.3200	0.6462	0.6060	0.6123	0.7046	5.43%
LS+L-PTS	k.v.gate.down	8.0821	0.8352	0.7174	0.7867	0.7992	0.4898	0.5651	0.3260	0.6643	0.6322	0.6262	0.7108	3.56%
LS+L-PTS + VAR	all	9.4983	0.7872	0.6606	0.7606	0.7601	0.4334	0.5372	0.2880	0.6390	0.5532	0.5729	0.6689	10.60%
LS+L-PTS + VAR	k.o.gate.down	8.2930	0.8116	0.7135	0.7851	0.7908	0.4838	0.5634	0.3300	0.6498	0.6095	0.6189	0.7079	4.64%
LS+L-PTS + VAR	k.v.gate.down	8.0259	0.8306	0.7269	0.7851	0.7955	0.4863	0.5673	0.3260	0.6715	0.6327	0.6317	0.7143	3.36%